Evidence of Polycomb-independent Catalysis of Histone H3 Lysine 27 Trimethylation

by

Lorenza Donnelly

An honors thesis submitted in partial fulfillment

of the requirements for graduation with Honors in the degree of

Bachelors of Science in Cellular and Molecular Biology

at the University of Michigan

May 2014

Sponsor:
Sundeep Kalantry, PhD.
Assistant Professor
Department of Human Genetics
University of Michigan Medical School

TABLE OF CONTENTS

ABSTRACT

Transcriptional regulation can occur through the modification and remodeling of chromatin, which consists of DNA, histones, and non-histone proteins. One such mechanism that controls gene expression is the chemical modification of histones. The Polycomb repressive complex 2 (PRC2) is a histone-modifying complex that catalyzes the trimethylation of lysine 27 on histone H3 (H3K27me3), a modification that is associated with transcriptional repression. PRC2 consists of the core proteins EZH2, EED, and SUZ12, along with other co-factors. Essential insights into PRC2 function have occurred through the study of its involvement in X-chromosome inactivation. X-inactivation is an epigenetic phenomenon by which female mammals achieve dosage compensation by silencing genes on one of two X chromosomes. PRC2 core proteins as well as H3K27me3 are physically enriched on the inactive X-chromosome. Our lab has found, however, that in mouse extra-embryonic endoderm (XEN) cells, H3K27me3 accumulates on the inactive-X independently of EZH2 enrichment. I tested whether H3K27me3 would still be enriched on the inactive-X of XEN cells devoid of EZH2, and I discovered that H3K27me3 enrichment on the inactive-X still occurs in *Ezh2*$^{-/-}$ XEN cells. I next tested whether EZH1, a homolog of EZH2, is responsible for this residual H3K27me3, and I found that while enrichment of H3K27me3 on the inactive-X was ablated in *Ezh2*$^{-/-}$;*Ezh1*$^{-/-}$ XEN cells, global levels of H3K27me3 were unaffected when compared to *Ezh2*$^{-/-}$ XEN cells by Western blotting. Additionally, I observed a similar outcome in *Eed*$^{-/-}$ XEN cells. These data suggest that although PRC2 is required for enrichment of H3K27me3 on the inactive-X, a PRC2-independent histone methyltransferase is capable of catalyzing H3K27me3 in XEN cells.

INTRODUCTION

Chromatin is composed of more than just the condensed DNA sequence that contains the genetic information necessary for life. In addition to DNA, chromatin consists of nucleosomes, which are octamers composed of 4 types of core histones around which DNA is wrapped, as well as non-histone proteins, which include chromatin-modifying enzymes. Each of the core histones, H2A, H2B, H3, and H4, contains an N-terminal unstructured domain, or “tail,” which projects outside of the structure of the nucleosome and is subject to post-translational modifications. Histone tails can be methylated, acetylated, phosphorylated, or subject to addition of other chemical groups by histone-modifying enzymes.

Modifications or combinations of modifications on specific histone residues are often associated with distinct transcriptional states of the surrounding genes, including active and repressed transcriptional states. It is typically thought that histone modifications function either by changing the level of compaction of chromatin or by recruiting downstream non-histone proteins that may then impact transcription (Shogren-Knaak et al., 2006). For these reasons, as well as the fact that histone modifications persist from one cell cycle division to the next, histone modifications have been proposed to be carriers of epigenetic information (Kouzarides 2007).

Epigenetics is the study of stable, heritable changes in transcription that occur independently of alterations in the DNA sequence, and epigenetic regulation is now recognized as playing a key role both during development and in disease. Although it has yet to be fully determined whether histone modifications are capable of

autonomously transmitting the epigenetic memory, it is widely believed that they are involved in epigenetic processes (Kouzarides 2007).

The Polycomb repressive complex 2 (PRC2) is a complex of proteins thought to be involved in epigenetically silencing genes. PRC2 catalyzes the trimethylation of lysine 27 on histone H3 (H3K27me3). This histone mark is thought to help recruit downstream factors that contribute to a silenced transcriptional state (Cao et al., 2002, Margueron et al., 2011). It was first suspected that PRC2 could play a role in epigenetic regulatory pathways when in *Drosophila,* embryos devoid of Esc (known as EED in mammals), a core member of PRC2, displayed a paradoxical phenotypic outcome. Based on the study of these temperature-sensitive *esc*$^{-/-}$ embryos, in which loss of Esc could be observed at various time points, researchers found that Esc is only required for developmental fate determination during a discrete window of time during early embryogenesis. Interestingly, the defect exhibited in these mutant embryos was at a much later stage of embryogenesis than the window of time in which Esc was missing during early embryogenesis. Loss of Esc at the later periods of development did not result in a defect, despite the fact that Esc is expressed constitutively throughout development (Struhl and Brower 1982). These results suggest that Esc acts to establish a transcriptional state of homeotic genes allowing for proper developmental fate determination, which can be maintained regardless of the presence or absence of Esc after that point, suggesting a memory effect. Additionally, PRC2 as a whole further fits the profile of an epigenetic regulator because it is allosterically activated by binding to the mark it catalyzes (via the EED subunit), providing an intrinsic mechanism for propagation and maintenance of H3K27me3 at target sites (Margueron et al., 2009).

The core members of mammalian PRC2 are EZH2, SUZ12, and EED, which correspond to E(z), Suz12, and Esc in *Drosophila*, respectively (Figure 1). EZH2 is the catalytic subunit that methylates histone H3 through its SET domain (Muller et al., 2002). In *Drosophila*, E(z), the H3K27me3 methyltransferase, is a single protein, but in mammals, it exists in the form of two homologs: EZH2 and EZH1 (Laible et al., 1997). Although the methyltransferase activity of EZH2 is better characterized, EZH1 also contains a SET domain, and there has been speculation as to whether it can form an alternative PRC2 complex and catalyze H3K27me3 (Shen et al., 2008, Margueron et al., 2008).

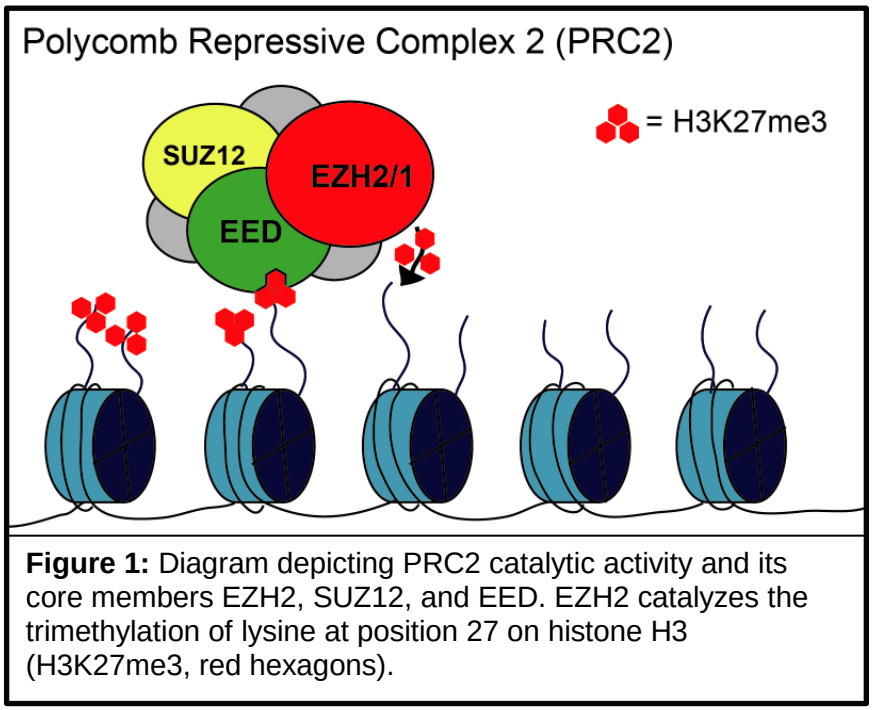

Figure 1: Diagram depicting PRC2 catalytic activity and its core members EZH2, SUZ12, and EED. EZH2 catalyzes the trimethylation of lysine at position 27 on histone H3 (H3K27me3, red hexagons).

Despite not possessing intrinsic methyltransferase activity, EED, a WD40-repeat protein, is arguably the most central component of PRC2. E(z) and EZH2, on their own, have been shown to be catalytically deficient, requiring interaction with both Esc/EED and Suz12 for robust methylation activity (Kuzmichev et al., 2002, Simon and Kingston 2009). As demonstrated in an *in vitro* pull-down assay, EED coordinates binding of EZH2 to the other PRC2 components (including SUZ12), since EZH2 does not directly interact with any of the other core proteins. At a minimum, interaction with EED and

SUZ12 is necessary for EZH2 to manifest its full methyltransferase potential (Cao and Zhang 2004). Deletion of any of the WD40 repeats after the first 81 amino acids of EED results in abolishment of the EED-EZH2 interaction (Cao et al., 2014). Additionally, another study in *Drosophila* has shown that functional Esc is necessary for E(z) catalytic activity even in the presence of an interaction between the two proteins, as formation of a complex containing a partial mutant Esc protein that still contains the WD40 domains for binding E(z), but lacks its N-terminal domain, results in loss of methyltransferase activity (Tie et al., 2007). More directly, researchers have shown that in *Eed*$^{-/-}$ mouse embryonic stem (ES) cells, H3K27me3 is depleted in both immunofluorescence (IF) assays and Western blotting (Montgomery et al., 2005). Thus, EED is necessary for both the formation and catalytic function of the PRC2 complex. As such, *Eed*$^{-/-}$ embryos and cells have commonly been thought of as being effectively "PRC2 null."

In addition to its known roles in genome-wide histone methylation, PRC2 is also known to be involved in the epigenetic process of X-chromosome inactivation. X-inactivation, a form of dosage compensation that occurs in mammals, is the phenomenon by which XX female mammals globally transcriptionally silence one of two X chromosomes in order to equalize X-linked gene expression with XY males. Once the inactive-X (Xi) in a given cell has been chosen and silenced during development, with few exceptions, it maintains the silent state through mitosis for the remainder of the animal's life (Lyon 1961, Payer and Lee 2008). X-inactivation is stably maintained in the somatic cells of all female mammals, thus making it an important model system for the study of epigenetic mechanisms and cell memory. The involvement of PRC2 in X-inactivation was first discovered when it was found that in the extra-embryonic portion of

Eed$^{-/-}$ embryonic day (E) 7.5 mouse embryos carrying an X^{GFP} transgene, the inactive-X was aberrantly re-activated (Wang et al., 2001).

PRC2 proteins are thought to be recruited to the inactive-X through the X-linked long noncoding RNA Xist (X-inactive specific transcript), which is expressed specifically from the inactive-X (Brown et al., 1991). The RNA physically coats the inactive-X, a phenomenon that can be visualized through the use of RNA fluorescence *in situ* hybridization (RNA FISH). Transgenic expression of Xist in male ES cells is sufficient to recruit PRC2 to the X chromosome, and expression of a mutant version of Xist containing a large inversion spanning much of the gene in female blastocyst stage mouse embryos is no longer capable of PRC2 recruitment to the Xist-coated X chromosome (Plath et al., 2003, Silva et al., 2003). Furthermore, Xist has recently been shown to target Jarid2, a PRC2 cofactor, to the inactive-X chromosome (da Rocha et al., 2014). Although the mechanism remains unclear, Xist potentially provides a means for PRC2 to get to the inactive-X chromosome during X-inactivation.

PRC2 components such as EZH2 and EED accumulate on the inactive-X along with Xist during early mouse embryogenesis, as assessed by immunocytochemistry; accordingly, H3K27me3 is also found enriched on the inactive-X in early embryos (Silva et al., 2003, Kalantry et al., 2006). Co-localization of H3K27me3 with the Xist RNA coat can therefore be used as a readout of PRC2 activity (Figure 3).

Both X-inactivation and Polycomb group function have also been well-studied in mouse stem cell lines. Several types of stem cell lines can be derived from E3.5 mouse blastocyst-stage embryos: these include extra-embryonic endoderm stem (XEN) cells, trophoblast stem (TS) cells, and mouse embryonic stem (ES) cells (Figure 2). XEN, TS, and ES cells derive from the portions of the blastocyst that go on to become the yolk sac, placenta, and the fetus, respectively. When stained via IF using antibodies against EZH2 and H3K27me3, combined with RNA FISH for Xist RNA, TS cells resemble blastocyst-stage embryos in that Xist, H3K27me3, and EZH2 are all enriched on the inactive-X (Plath et al., 2003). In XEN cells, however, while Xist and H3K27me3 accumulate on the inactive-X, EZH2 is not enriched on the inactive-X (Figure 3).

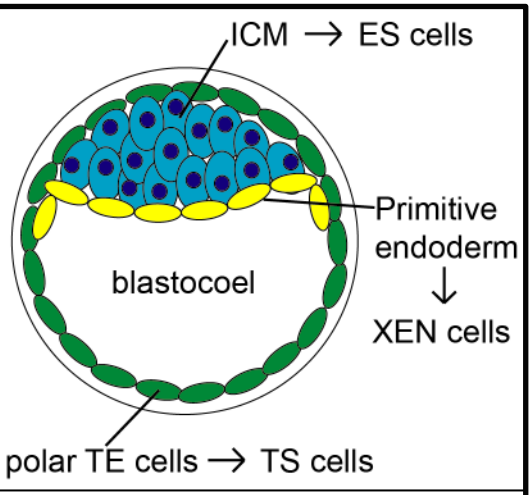

Figure 2: Diagram of a mouse blastocyst (E3.5), from which XEN, TS, and ES cells can be derived.

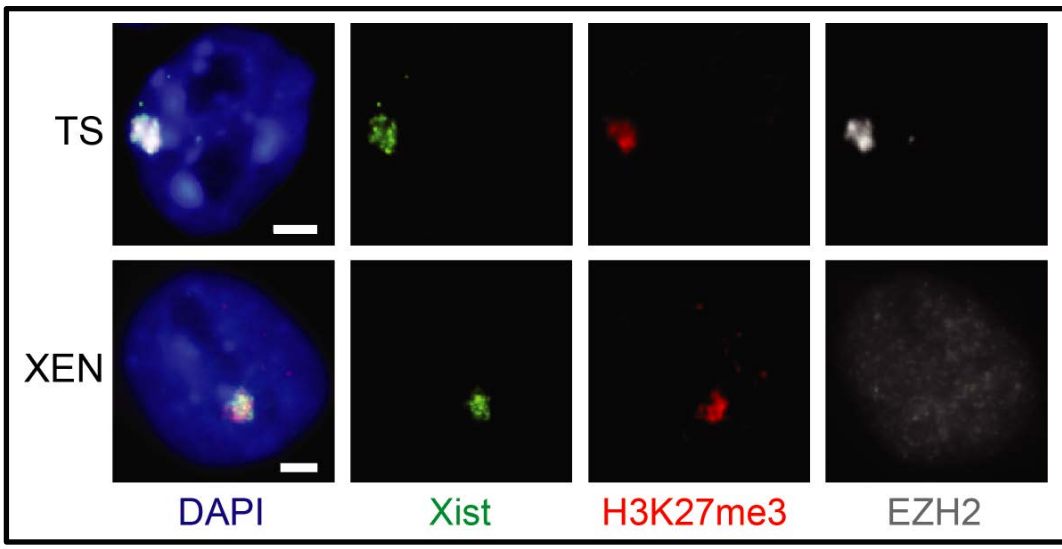

Figure 3: IF/FISH staining of Xist, H3K27me3, and EZH2 in representative wild-type female TS and XEN cells. Nuclei are stained with DAPI. Scale bars, 2.5 μm.

Because of the lack of enrichment of EZH2 on the inactive-X as assessed by IF, we questioned whether another factor could also catalyze H3K27me3 on the inactive-X in XEN cells. We therefore decided to investigate the requirement for various core components of PRC2 for catalysis of H3K27me3. Our hypothesis is that a methyltransferase other than EZH2 can catalyze H3K27me3.

This study is significant because in addition to providing insights into factors that contribute to the catalysis of the repressive histone modification H3K27me3, which is intrinsically of interest to chromatin biologists; the results can also be linked to more translational aspects, such as cancer therapy. Researchers have observed overexpression of EZH2, and consequently increased levels of H3K27me3, in various forms of cancer, including prostate and breast cancer (Varambally et al., 2002, Kleer et al., 2003). As such, inhibitors of EZH2 aimed at decreasing H3K27me3 levels, and hence potentially ameliorating the negative effects of high levels of H3K27me3, have been brought forward as cancer therapeutic agents (McCabe et al., 2012). If, however, there are EZH2-independent, or even PRC2-independent, pathways of H3K27me3 catalysis, these therapies may not be fully effective in the treatment of cancer.

RESULTS AND DISCUSSION

H3K27me3 catalysis in *Ezh2*$^{-/-}$ XEN cells

In order to be able to examine the extent to which H3K27me3 is catalyzed in the absence of EZH2, a member of the lab generated *Ezh2* mutant XEN cells for analysis (Clair Harris, Acknowledgements). To generate *Ezh2*$^{-/-}$ XEN cells, we first derived conditionally-mutant *Ezh2*$^{fl/fl}$ XEN cells (Su et al., 2002). The XEN cell lines were generated from embryonic day (E) 3.5 mouse embryos in which exons 15-18, which encode the SET domain, are flanked by *loxP* sites (*Ezh2*$^{fl/fl}$). Since the SET domain is the catalytic unit of EZH2, deletion of the SET domain ensures that regardless of whether a truncated protein is expressed, the mutation is null. Female *Ezh2*$^{fl/fl}$ XEN cells were then transfected with Cre recombinase to delete the floxed exons, generating a null allele (*Ezh2*$^{-/-}$) (Figure 4). This strategy allows for direct comparison of parent cell lines in which *Ezh2* is still present (*Ezh2*$^{fl/fl}$) to the derivative cell line that is *Ezh2* null (*Ezh2*$^{-/-}$).

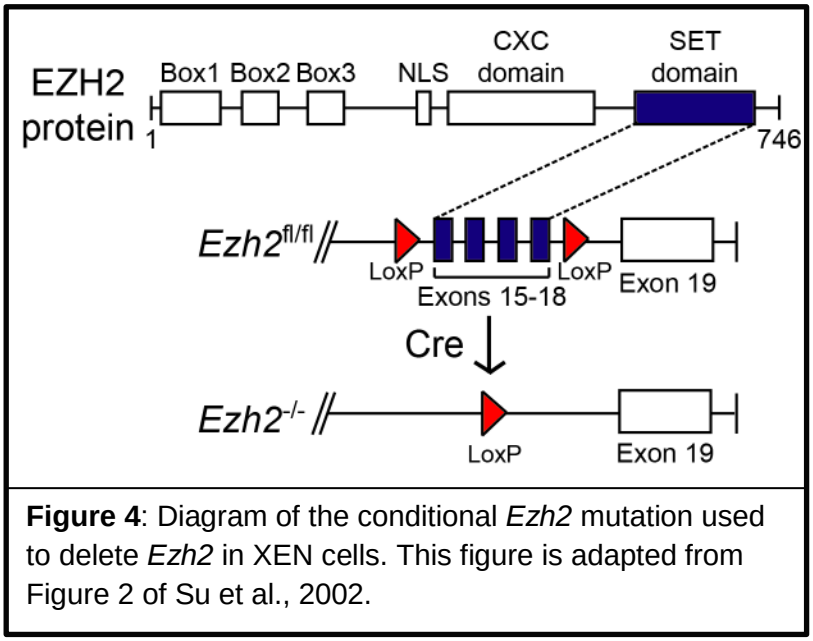

Figure 4: Diagram of the conditional *Ezh2* mutation used to delete *Ezh2* in XEN cells. This figure is adapted from Figure 2 of Su et al., 2002.

Using genomic PCR, RT-PCR, and Western blotting, I validated that *Ezh2* had been properly deleted in the *Ezh2*$^{-/-}$ XEN cells (Figure 5a-c). The *Ezh2* deletion produces a truncated RNA (Figure 5b), but does not produce a stable truncated protein,

as Western blotting using a monoclonal antibody against the residues of EZH2 surrounding Arg354 (which corresponds to a region that is encoded for by a region of the gene that remains intact in the mutant allele) did not detect a shorter band (Figure 5d), and the lack of a truncated protein in this mutant allele has also been previously reported (Su et al., 2002).

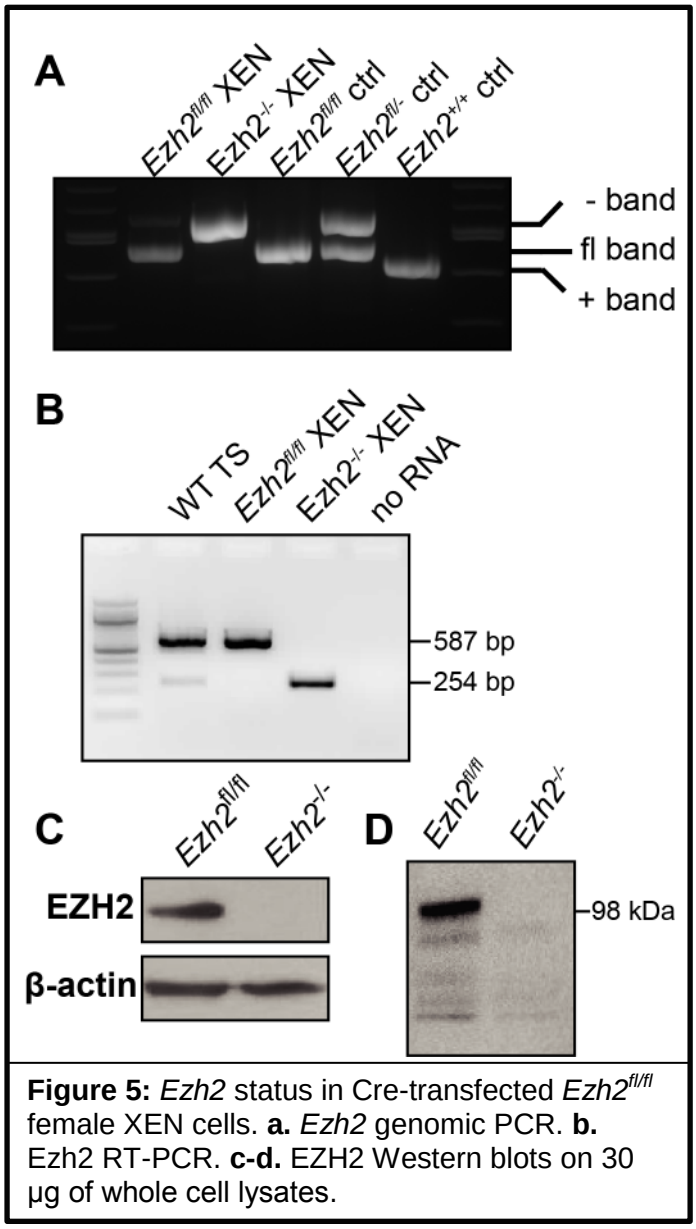

Figure 5: *Ezh2* status in Cre-transfected *Ezh2*$^{fl/fl}$ female XEN cells. **a.** *Ezh2* genomic PCR. **b.** Ezh2 RT-PCR. **c-d.** EZH2 Western blots on 30 µg of whole cell lysates.

Having verified that *Ezh2* had been homozygously deleted and that no protein is made following Cre transfection of the XEN cells, I performed H3K27me3 IF followed by Xist RNA FISH to assess whether H3K27me3 would accumulate on the inactive-X in the absence of EZH2 (Figure 6a). For this analysis, I used three different antibodies against H3K27me3 (Millipore, Active Motif, and Abcam). Quality control experiments by the manufacturers, as well as by other groups, suggests that these antibodies are highly specific and detect only H3K27me3 (Egelhofer et al., 2011). I counted three sets of 100 nuclei for each antibody in each cell line to quantify how often H3K27me3 was enriched on the inactive-X; the

inactive-X is marked by Xist RNA accumulation (Figure 6b). For the two antibodies with better staining efficiency in *Ezh2*$^{fl/fl}$ XEN cells (Millipore and Active Motif), the percentage of nuclei with accumulation of H3K27me3 on the inactive-X in *Ezh2*$^{-/-}$ XEN cells remained approximately the same as for *Ezh2*$^{fl/fl}$ XEN cells, although staining intensity throughout the nucleus was somewhat reduced (Figure 6b and data not shown). The third antibody (Abcam), however, which stained the inactive-X poorly even in *Ezh2*$^{fl/fl}$ XEN cells (at an efficiency of about 50% of Xist-coated nuclei), did not show accumulation of H3K27me3 on the inactive-X in *Ezh2*$^{-/-}$ XEN cells (Figure 6b).

Because of this slight discrepancy between the different H3K27me3 antibodies, I decided to assess global levels of H3K27me3 in *Ezh2*$^{-/-}$ XEN cells. I extracted histones from *Ezh2*$^{fl/fl}$ and *Ezh2*$^{-/-}$ XEN cells and performed Western blotting against H3K27me3. For all three antibodies, H3K27me3 was detectable by Western blotting in the absence of EZH2, albeit at lower levels compared to the control cell line (Figure 6c). This confirms the results from the IF/ RNA FISH experiments. The findings further suggest that the lack of staining observed with the Abcam antibody is because of a decrease in the amount of H3K27me3; this antibody stains relatively weakly and is unable to detect the lower levels of H3K27me3 on the inactive-X by IF in the mutant cells. Nevertheless, from these data, it appears that despite the absence of EZH2 protein, H3K27me3 is able to be catalyzed and is still enriched on the inactive-X.

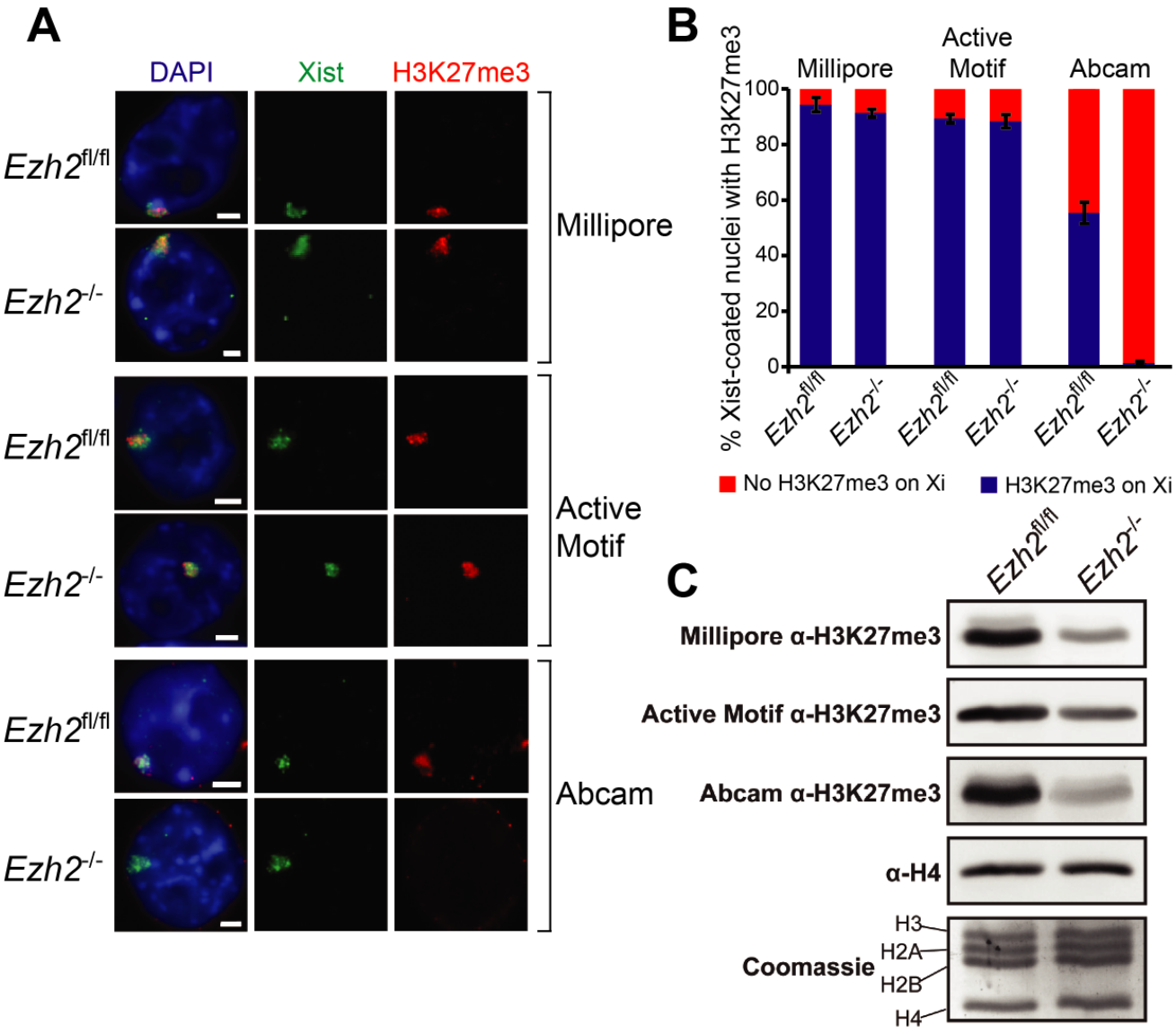

Figure 6: **a.** Immunofluorescence detection of H3K27me3 using three different antibodies in *Ezh2*$^{fl/fl}$ and *Ezh2*$^{-/-}$ female XEN cells. Xist RNA FISH marks the inactive-X. Scale bars, 2.5 μm. **b.** Quantification of Xist and H3K27me3 co-localization for Xist-coated nuclei. Mean ± standard error, n=300 (3 separate stains counted for 100 nuclei each). **c.** Histone extracts from *Ezh2*$^{fl/fl}$ and *Ezh2*$^{-/-}$ XEN cells analyzed by Western blotting for H3K27me3 using the three antibodies, as well as a histone H4 antibody and Coomassie staining of the histone extracts.

H3K27me3 catalysis in *Ezh2*$^{-/-}$;*Ezh1*$^{-/-}$ XEN cells

Because of previous studies suggesting that EZH1, the homolog of EZH2, may have catalytic activity as part of PRC2 (Shen et al., 2008), we decided to investigate whether the residual H3K27me3 observed in *Ezh2*$^{-/-}$ XEN cells is attributable to EZH1 taking the place of EZH2 in PRC2-mediated catalysis of H3K27me3. We therefore generated *Ezh2*$^{fl/fl}$;*Ezh1*$^{-/-}$ XEN cells and transfected the derived cells with Cre to yield *Ezh2*$^{-/-}$;*Ezh1*$^{-/-}$ XEN cells. Since the nature of this *Ezh1* mutation has not been previously published (Acknowledgements), I characterized the genomic sequence of the construct by using a series of PCR primers and sequencing products. EZH1 has 21 exons, of which exon 17 through half of exon 21 constitute the SET domain (Figure 7). The mutation consists of a 750 bp deletion in the middle of exon 7 extending into intron 7-8, followed by an insertion containing a β-geo cassette and other vector sequences.

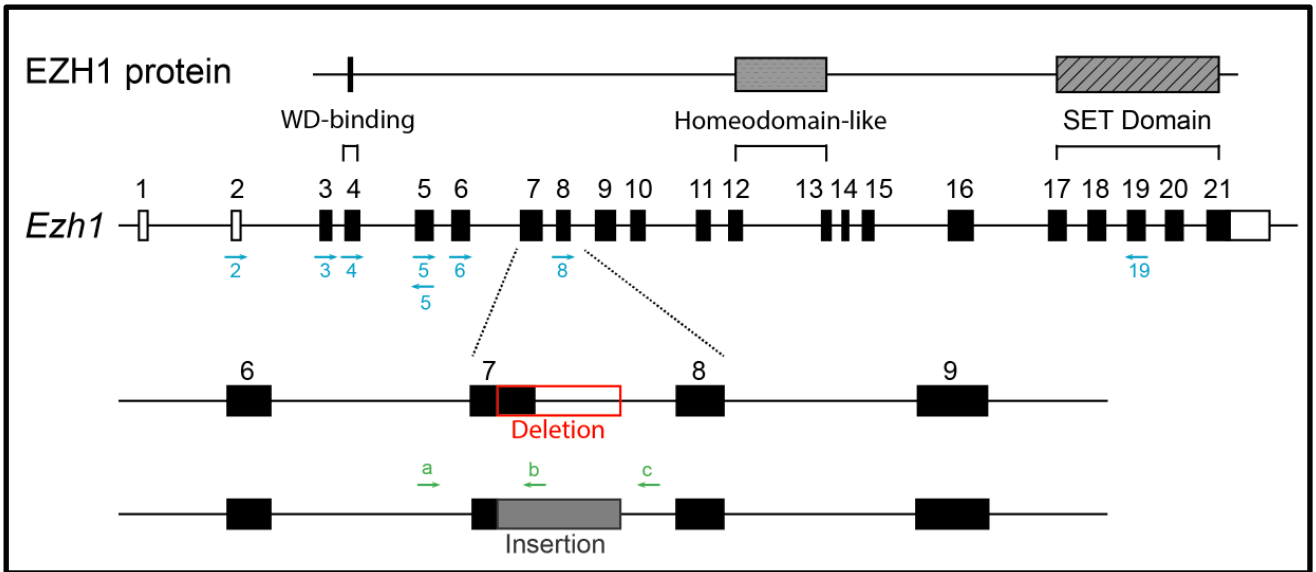

Figure 7: Diagram of the *Ezh1* mutation used in this study. RT-PCR primers are shown as blue arrows, and genotyping primers are shown as green arrows (diagram created by Clair Harris)

Using *Ezh2*$^{fl/fl}$;*Ezh1*$^{-/-}$ mice to generate E3.5 embryos, we derived two *Ezh2*$^{fl/fl}$;*Ezh1*$^{-/-}$ XEN cell lines, one male and one female. The lines were then transfected with Cre to induce conditional deletion of *Ezh2.* To verify the genotypes of the lines, I performed *Ezh2* and *Ezh1* genomic PCRs on the cell lines (Figure 8). I furthermore performed an Ezh1 RT-PCR on the cell lines in order to assess whether there was any transcription from the mutant allele, as well as Ezh2 RT-PCRs for genotyping purposes (Figure 9a). The *Ezh1* mutation produces a truncated mRNA that is transcribed until the middle of Exon 7, where the deletion begins (Figure 9b). There are some instances where faint bands can be detected by using primers in scattered regions downstream of the deletion, but I did not find evidence of a continuous transcript that would produce a sizable protein, as assessed by RT-PCR primer pairs and 5'RACE (Figure 9c and data not shown).

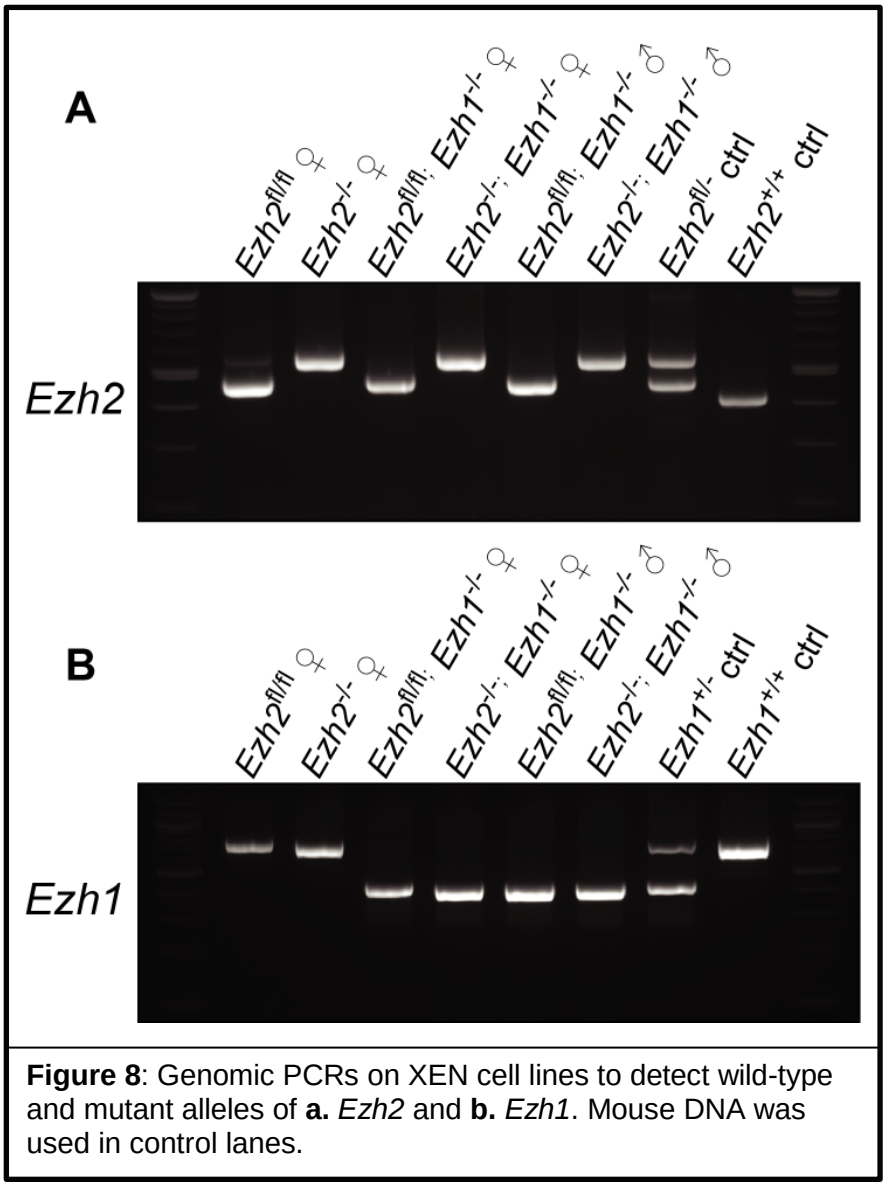

Figure 8: Genomic PCRs on XEN cell lines to detect wild-type and mutant alleles of **a.** *Ezh2* and **b.** *Ezh1*. Mouse DNA was used in control lanes.

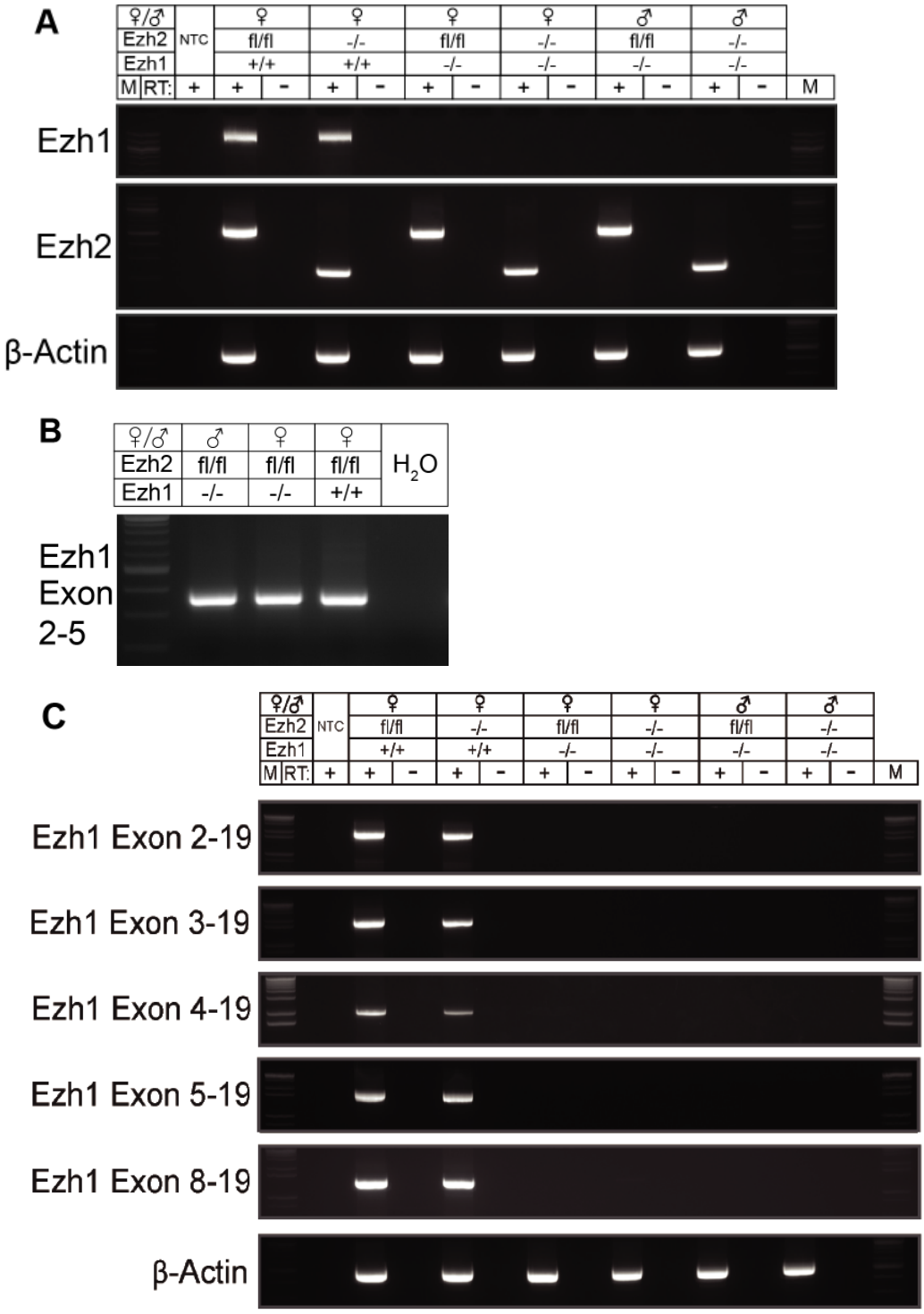

Figure 9: Verification of *Ezh1* mutant XEN cells by RT-PCR analysis. **a.** Ezh1 RT-PCR using primers in exons 6 and 19, and Ezh2 RT-PCR to demonstrate genotypes of cells. **b.** RT-PCR using primers in exons 2 and 5 of Ezh1 to show presence of the truncated mRNA transcript. **c.** Various primer sets showing lack of a continuous transcript in *Ezh1* mutant XEN cells. Additional primer sets were also tested (data not shown). Figures 9A and 9C made by Clair Harris.

To check for protein products in the various mutant cell lines, I performed Western blotting for EZH2 (Figure 10). Unfortunately, the level of endogenous EZH1 protein appears to be too low in XEN cells to be detectable by Western blotting, based on my tests of six different antibodies against EZH1 (Methods, Table 1). Because of this, I have not been able to unequivocally show that there is no EZH1 protein in the *Ezh1*$^{-/-}$ XEN cells. However, based on the RT-PCR data, it would be impossible for there to be a full-length protein, and the SET domain is on the C-terminal end of the protein (which is after the deletion and insertion), making it unlikely that any potential methyltransferase activity of

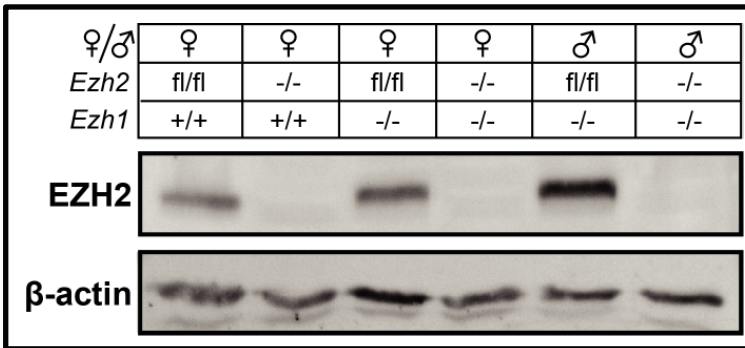

Figure 10: EZH2 Western blot using 30 µg of whole cell lysates from XEN cell lines.

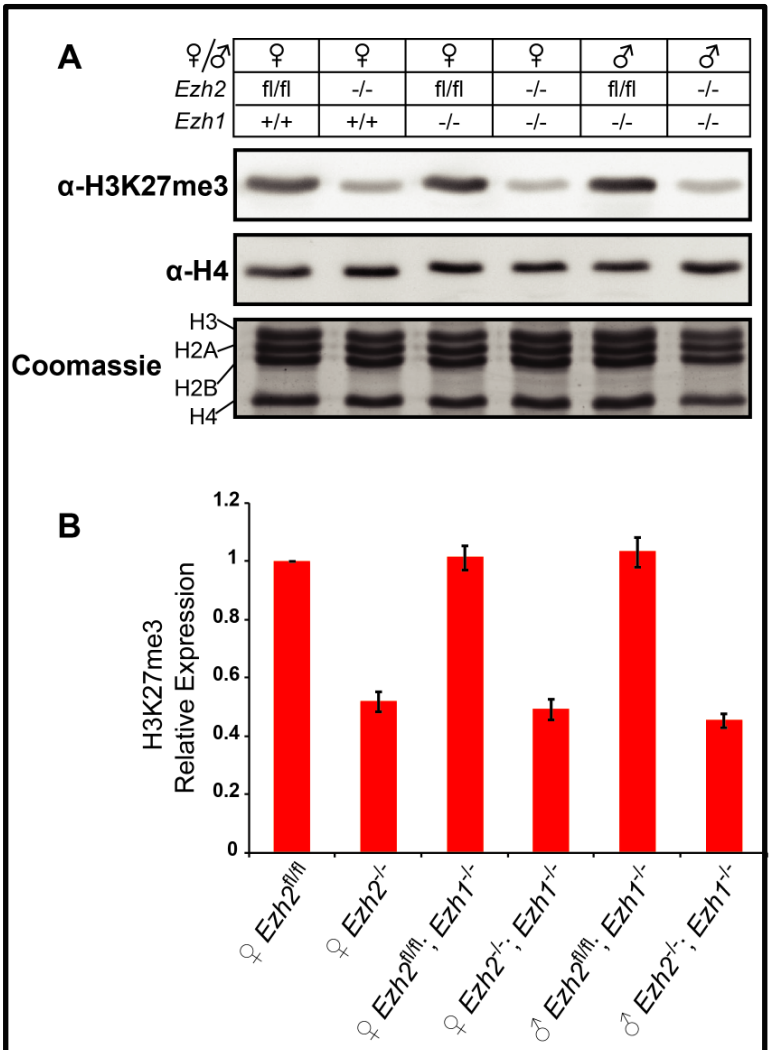

Figure 11: a. H3K27me3 Western blot using Millipore antibody, with histone H4 as a loading control and a Coomassie stain of histone preps. **b.** Quantification of band intensity, normalized to histone H4 loading control. Mean ± standard error, n=3.

EZH1 would remain functional in these cells, even if a shortened protein were made from the first seven exons.

I then repeated the same set of analyses for H3K27me3 detection as in the *Ezh2*$^{-/-}$ single mutant XEN cells with our best antibody (Millipore). Surprisingly, H3K27me3 was still detectable by Western blotting even in *Ezh2*$^{-/-}$;*Ezh1*$^{-/-}$ XEN cells (Figure 11a). The H3K27me3 and histone H4 Western blots were done using fluorescent secondary antibodies simultaneously in two different channels, and they were imaged in a SynGene G:Box gel-doc system. The use of this system, as well as its associated software, allows for accurate quantification of the fluorescent signal that does not rely on the use of scanning films. Using this quantification method, I determined that the amount of H3K27me3 in double mutant cells appeared to be the same as in *Ezh2*$^{-/-}$ single mutant XEN cells (Figure 11b).

When I performed IF/ Xist RNA FISH on the *Ezh2*$^{-/-}$;*Ezh1*$^{-/-}$ double mutant cells, however, there was no detectable enrichment of H3K27me3 with Xist on the inactive-X (Figure 12a-b). There was still background staining present for H3K27me3, however, and in some instances, nuclei took on a “speckled” appearance in which there were multiple foci of high DAPI staining intensity, and the H3K27me3 often co-localized with the DAPI foci in these instances, but not with the inactive-X (Figure 12c). These data suggest that in the absence of both EZH2 and EZH1, H3K27me3 is still catalyzed in XEN cells, but that specific enrichment of H3K27me3 on the inactive-X is impaired. This implies that targeting of H3K27me3 to the inactive-X requires either EZH2 and/or EZH1. This supports the idea that Xist RNA directly or indirectly recruits PRC2 in order to cause enrichment of H3K27me3 on the inactive-X chromosome.

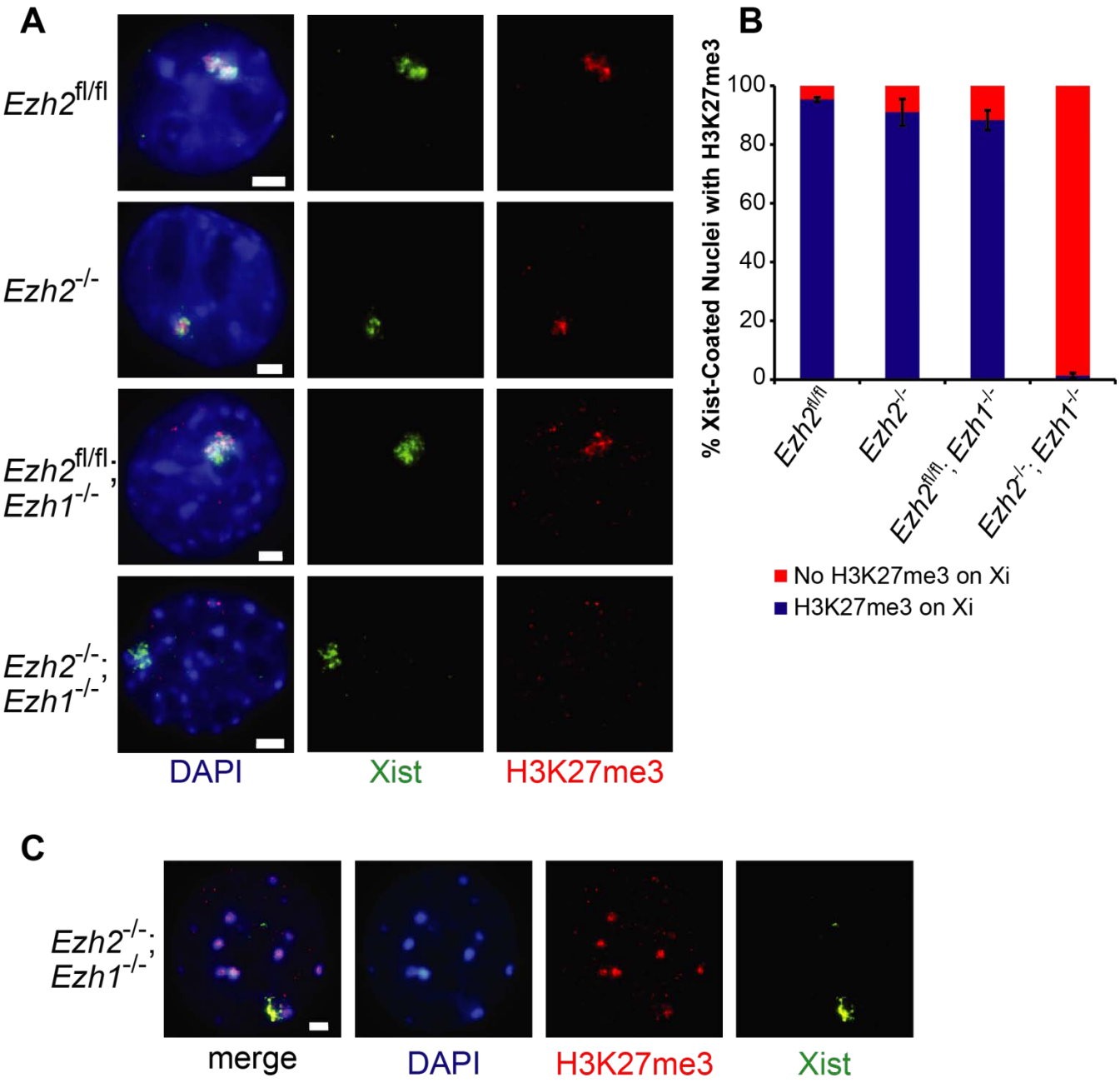

Figure 12: a. Immunofluorescence detection of H3K27me3 using the Millipore antibody in *Ezh2*$^{fl/fl}$, *Ezh2*$^{-/-}$, *Ezh2*$^{fl/fl}$;*Ezh1*$^{-/-}$, and *Ezh2*$^{-/-}$;*Ezh1*$^{-/-}$ female XEN cells. Xist RNA FISH marks the inactive-X. **b.** Quantification of H3K27me3 on Xist-coated nuclei. Mean ± standard error, n=300 for three separate counts of 100 nuclei each. **c.** Representative image of a subset of nuclei that display H3K27me3 localization on spots of high DAPI staining intensity. Scale bars, 2.5 μm.

H3K27me3 catalysis in *Eed*$^{-/-}$ XEN cells

Since H3K27me3 was still present in *Ezh2*$^{-/-}$;*Ezh1*$^{-/-}$ XEN cells, we wished to know if H3K27me3 is catalyzed in *Eed*$^{-/-}$ XEN cells. Previous work showed a complete absence of H3K27me3 in *Eed*$^{-/-}$ ES cells (Montgomery et al., 2005). We therefore hypothesized that another methyltransferase, instead of EZH2 or EZH1, might be associating with EED in order to catalyze H3K27me3. We therefore decided to generate *Eed*$^{-/-}$ XEN cells in order to test whether H3K27me3 would be abolished, which would be consistent with the hypothesis that the methyltransferase responsible for residual H3K27me3 in the *Ezh2*$^{-/-}$;*Ezh1*$^{-/-}$ XEN cells does so via association with EED. Using mice with the mutation construct shown in Figure 13, a member of the lab (Clair Harris, see Acknowledgements) generated female *Eed*$^{fl/-}$ and *Eed*$^{-/-}$ XEN cells (one parental *Eed*$^{fl/-}$ line and two *Eed*$^{-/-}$subclones after Cre transfection, #1 and #2) using a similar Cre transfection strategy as in the previous sections.

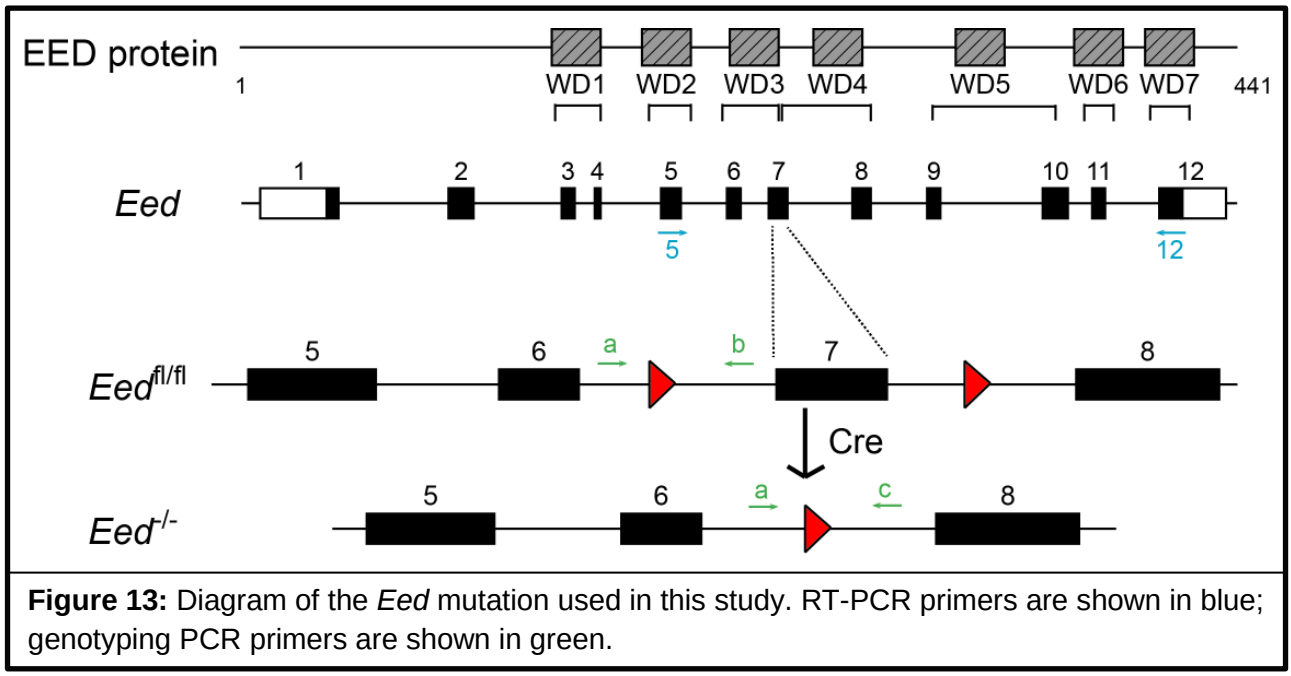

Figure 13: Diagram of the *Eed* mutation used in this study. RT-PCR primers are shown in blue; genotyping PCR primers are shown in green.

The *Eed* mutation used in this study results in a single exon deletion, exon 7, upon Cre transfection, as can be seen via PCR and RT-PCR (Figure 14a-b). Studies have shown that the WD40-repeat domains of EED are required for its interaction with EZH2 (Han et al., 2007). In fact, based on a series of truncation mutants, EED requires amino acids 90-441, which contain all of the 7 WD40 repeats, to interact with EZH2 (Sewalt et al., 1998). Expression of *Eed* constructs containing some, but not all, of the WD40 repeats results in a lack of interaction with EZH2 (Cao et al., 2014). Exon 7 (aa 212-242) encodes part of the 3rd and 4th WD40 repeats (aa 193-229 and 239-264); therefore, deletion of this exon should prevent formation of PRC2 even if a partial EED protein were to form (the sequence of the mutant mRNA was also analyzed, and there is a predicted in-frame stop codon created by the deletion).

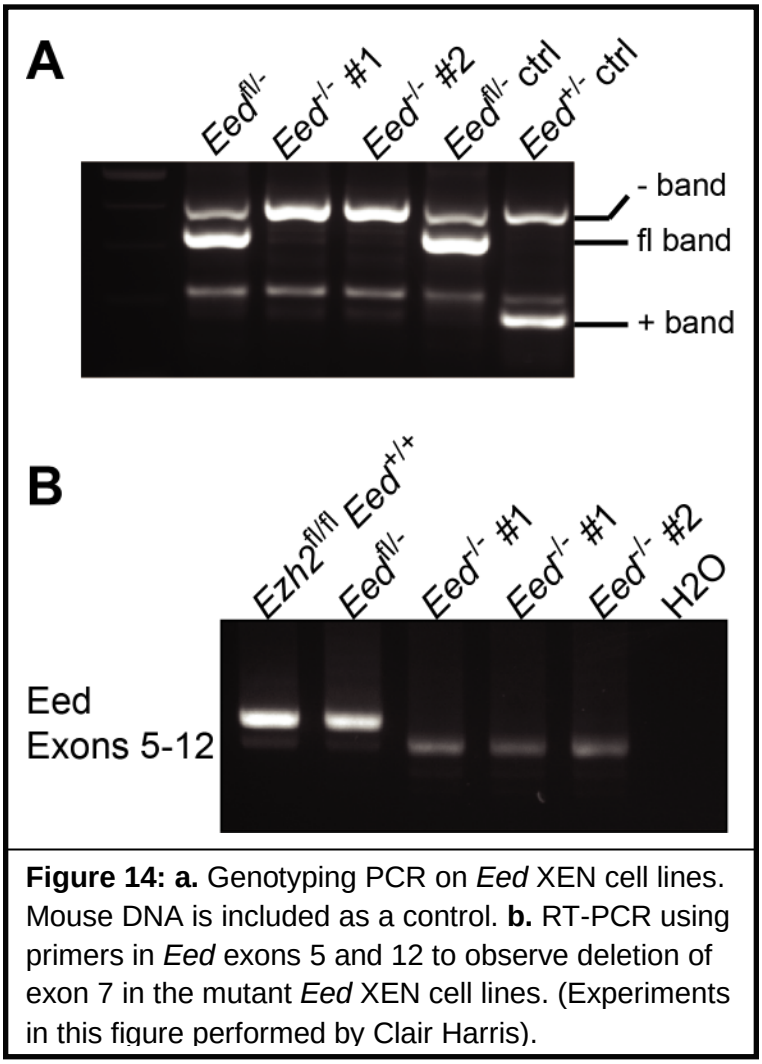

Figure 14: a. Genotyping PCR on *Eed* XEN cell lines. Mouse DNA is included as a control. **b.** RT-PCR using primers in *Eed* exons 5 and 12 to observe deletion of exon 7 in the mutant *Eed* XEN cell lines. (Experiments in this figure performed by Clair Harris).

I then analyzed levels of H3K27me3 in histone extracts from *Eed*$^{fl/-}$ and *Eed*$^{-/-}$ XEN cells by fluorescent Western blotting and quantification, as described in the

previous section (Figure 15a-b). Unexpectedly, I found that H3K27me3 was still present at significant levels in both *Eed*$^{-/-}$ XEN cell subclones.

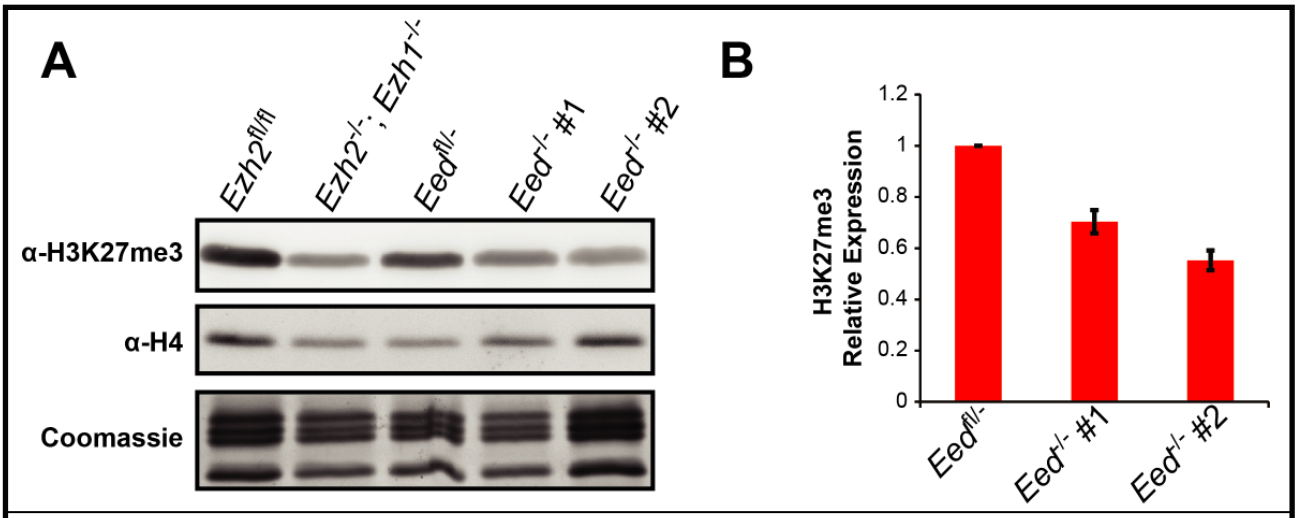

Figure 15: a. H3K27me3 Western blot using Millipore antibody, as well as an antibody against histone H4 and a Denville Blue Protein stain of histone preps as loading controls. **b.** Quantification of band intensity for *Eed*$^{fl/-}$ and *Eed*$^{-/-}$ XEN lines, normalized to H4 loading control. Mean ± standard error, n=4.

Similarly, I analyzed H3K27me3 catalysis on the inactive-X in *Eed*$^{fl/-}$ and *Eed*$^{-/-}$ XEN cells using H3K27me3 IF and Xist RNA FISH (Figure 16a). Just as in *Ezh2*$^{-/-}$*; Ezh1*$^{-/-}$ cells, loss of EED drastically reduced co-localization of H3K27me3 and Xist (Figure 16b). Based on this data, it appears that EED is necessary for accumulation of H3K27me3 on the inactive-X. This is in agreement with the data from the previous section, which showed that either EZH2 or EZH1 is necessary for localization of H3K27me3 to the inactive-X, but not for residual levels of global H3K27me3 catalysis. Taking these two sets of data together, the results are suggestive that PRC2 function is necessary for enrichment of H3K27me3 on the inactive-X, and that there is likely a PRC2-independent mechanism for catalysis of H3K27me3 in the absence of PRC2.

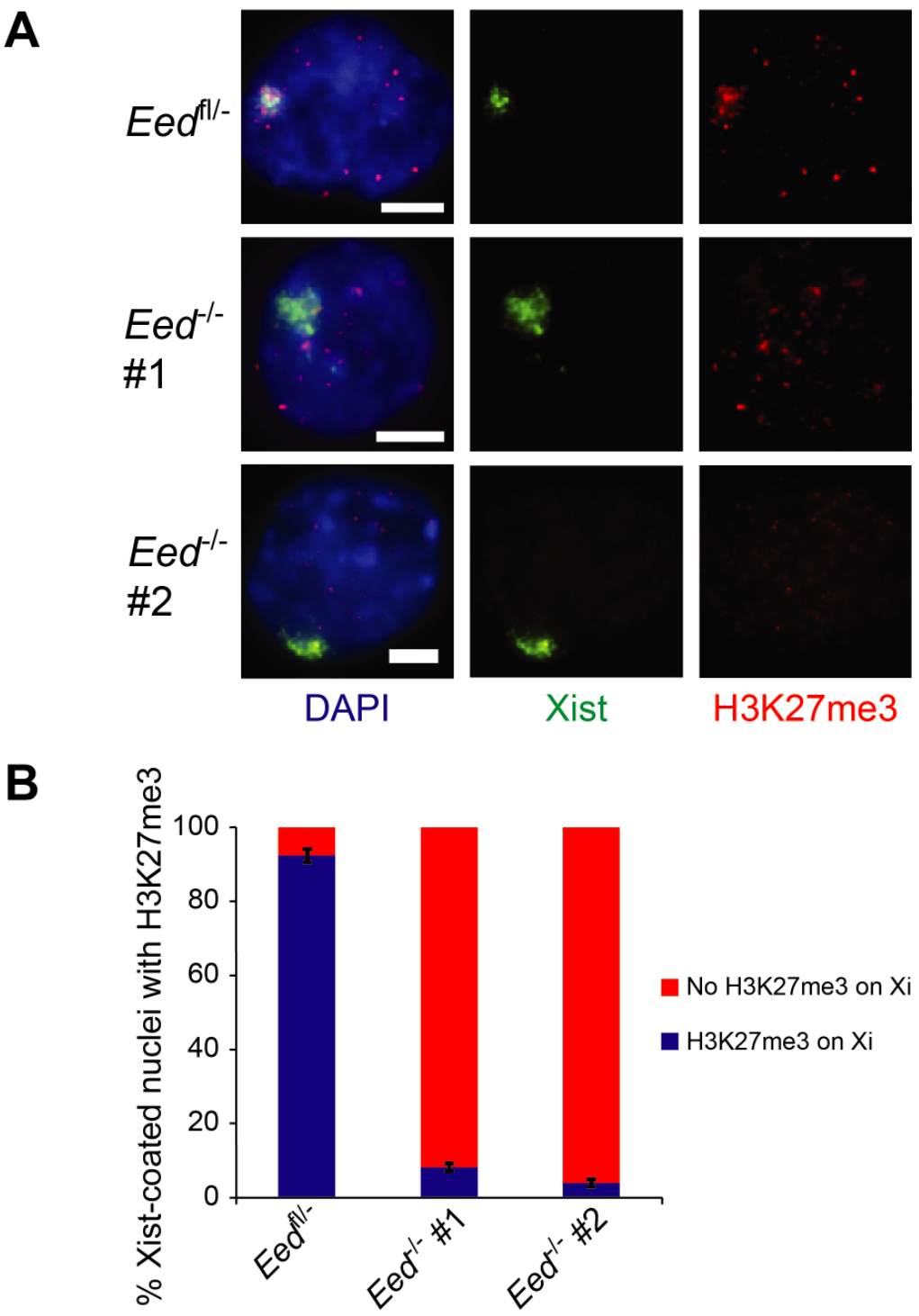

Figure 16: a. Immunofluorescence detection of H3K27me3 using the Millipore antibody in *Eed*$^{fl/-}$ and *Eed*$^{-/-}$ female XEN cells. Xist RNA FISH marks the inactive-X. **b.** Quantification of H3K27me3 on Xist-coated nuclei. Mean ± standard error, n=300 for three separate counts of 100 nuclei each for *Eed*$^{fl/-}$ and *Eed*$^{-/-}$ #2; n=500 for five separate counts for *Eed*$^{-/-}$ #1. Scale bars, 2.5 µm.

DISCUSSION

In this study, I assessed catalysis of the repressive histone mark H3K27me3 in the absence of Polycomb group proteins EZH2, EZH1, and EED in XEN cells. The results of this study demonstrate that, as assessed by IF, H3K27me3 is still enriched on the inactive-X in the absence of EZH2, and as assessed by Western blotting, H3K27me3 catalysis still occurs in the absence of EZH2, EZH2 together with EZH1, and EED. These results therefore imply that there is an unknown PRC2-independent factor capable of catalyzing H3K27me3.

Enrichment of H3K27me3 on the inactive-X is PRC2-dependent

The levels of H3K27me3 were similar between *Ezh2*$^{-/-}$ and *Ezh2*$^{-/-}$;*Ezh1*$^{-/-}$ XEN cells, which suggests that EZH1 does not contribute significantly to overall levels H3K27me3 catalysis in these cells. On the other hand, while single mutant *Ezh2*$^{-/-}$ and *Ezh1*$^{-/-}$ XEN cells showed no defects in levels or accumulation of H3K27me3 on the inactive-X, *Ezh2*$^{-/-}$;*Ezh1*$^{-/-}$ XEN cells lacked enrichment of H3K27me3 on the inactive-X. These data imply that EZH2 and/or EZH1 is required for inactive-X-specific accumulation of H3K27me3. *Eed*$^{-/-}$ XEN cells also lacked accumulation of H3K27me3 on the inactive-X, further cementing the idea that enrichment of H3K27me3 on the inactive-X is PRC2-dependent. These results are in agreement with the current model that Xist RNA may somehow target PRC2, and thereby H3K27me3, to the inactive-X. Further studies are necessary, however, to conclusively determine whether this is a direct interaction between Xist and PRC2 or an indirect effect caused by Xist expression, as recent studies disagree on which regions of Xist are necessary for PRC2

recruitment to the inactive-X, and reliable biochemical assays have yet to be performed (Da Rocha et al., 2014, Zhao et al., 2008).

The finding that H3K27me3 catalysis still occurred in *Ezh2*$^{-/-}$;*Ezh1*$^{-/-}$ XEN cells helps to elucidate the discrepancy between two previous studies that describe conflicting results on the requirement of EZH1 for residual H3K27me3 in Ezh2$^{-/-}$ ES cells (Shen et al., 2008, Margueron et al., 2008). In one study, residual H3K27me3 in *Ezh2*$^{-/-}$ ES cells was abolished upon Ezh1 siRNA treatment (Shen et al., 2008), while the other study found that H3K27me3 was still present in *Ezh2*$^{-/-}$ ES cells treated with Ezh1 siRNA (Margueron et al., 2008). In our study, H3K27me3 was clearly still catalyzed in *Ezh2*$^{-/-}$;*Ezh1*$^{-/-}$ cells, supporting the results of the second study. Furthermore, our use of a germline null *Ezh1* allele rather than siRNA allows for certainty of the depletion of EZH1 protein; in siRNA knockdown experiments, a complete knockdown of the protein of interest may not occur.

Presence of H3K27me3 catalysis in *Eed*$^{-/-}$ XEN cells

The finding that H3K27me3 was still catalyzed in *Eed*$^{-/-}$ XEN cells was highly unexpected, given previous data showing a lack of H3K27me3 in *Eed*$^{-/-}$ ES cells (Montgomery et al., 2005). There are several potential reasons as to the discrepancy between my results and previous data. Firstly, I believe that the fluorescent Westerns that I performed on purified histone extracts are more sensitive than the Western blots reported in previous studies. This idea is supported by the fact that even though others have reported H3K27me3 in the absence of EZH2 alone, the bands that I observe in my *Ezh2*$^{-/-}$ samples are much more robust compared to samples expressing EZH2 than in

analogous experiments in the literature (Shen et al., 2008, Margueron et al., 2008). Secondly, the previous studies resorted to examining ES cells; biochemical studies of ES cells are confounded by feeder cells that are required for proper growth and maintenance of the cell lines. In Westerns using ES cell lysates, faint bands can be attributed to feeder contamination, since it is difficult to ascertain that lysates are completely free of feeder cells. XEN cells do not require feeder cells for growth, allowing for the certainty that any H3K27me3 observed by Western blotting must be from the mutant XEN cells themselves.

Before definitive conclusions can be made, however, it will be necessary to conclusively show that there is no functional EED protein in our putative *Eed*$^{-/-}$ XEN cells, since there is a shortened, but not truncated, RNA produced in this cell line. Preliminarily, this shortened RNA is also less abundant than the wild-type Eed RNA. If, however, a shortened EED protein is produced from the mutant allele, I cannot exclude the possibility that this protein could be participating in the formation of the PRC2 complex, thus facilitating PRC2-dependent catalysis of H3K27me3. Arguing against this possibility, however, is the fact that our *Eed* mutation removes part of two WD40 repeats, and these WD40 domains have been shown to be required for EZH2 binding and EED function in the catalysis of H3K27me3 as part of PRC2 (Cao et al., 2014, Sewalt et al., 1998). If I do find evidence of a truncated protein in the *Eed*$^{-/-}$ XEN cells, I will need to perform immunoprecipitation to determine whether the PRC2 complex still forms. In this case, the H3K27me3-catalyzing methyltransferase could still be part of PRC2 and associate with the mutant EED protein. An EED immunoprecipitation could then be used to purify and identify the unknown methyltransferase.

A potential novel PRC2-independent histone methyltransferase capable of H3K27me3 catalysis

If I determine that there is no shortened EED protein in the *Eed*$^{-/-}$ XEN cells that is responsible for residual H3K27me3, then the presence of H3K27me3 in these cells implies the existence of a novel histone methyltransferase that catalyzes H3K27me3 in the absence of functional PRC2 components. The next step, then, would be to discover the identity of this methyltransferase. This process is complicated by the fact that in this case, the methyltransferase does not associate with EED, so there is no means of purifying it through interaction with EED. An alternative option is to examine known SET-domain containing proteins and use siRNA knockdown in both *Ezh2*$^{-/-}$ and *Ezh2*$^{-/-}$; *Ezh1*$^{-/-}$ XEN cells to look for whether knockdown of any of the proteins causes depletion of the residual H3K27me3 in these cell lines. To date, with only one exception, all lysine methyltransferases contain a SET domain, facilitating this approach (Dillon et al., 2005). Another potential method to identify the H3K27me3-catalyzing enzyme is an intensive column chromatography-based protein purification, using H3K27me3 activity as the readout of the purified proteins.

Whether or not the identity of the methyltransferase is discovered, this study is still significant in that it demonstrates the existence of H3K27me3 catalysis activity that is independent of EZH2, EZH1, and potentially EED. As such, it should not be expected that inhibition of EZH2 or EED in cancers that have a hyperabundance of the H3K27me3 mark will result in complete inhibition of H3K27me3 catalysis.

METHODS

Cell Lines

XEN cells were derived as described previously (Kalantry et al., 2006). Briefly, E3.5 embryos were flushed from the mouse uterus with medium (MEMα/10% fetal bovine serum) and plated individually on MEFs (mouse embryonic feeder cells) into wells of a 4-well tissue culture dish containing 750 µl of XEN derivation medium (MEMα, 50 µg/ml penicillin/streptomycin (Invitrogen, #15070063), 20% fetal bovine serum, 1 mM sodium pyruvate, 100 µM β-mercaptoethanol, 2mM L-glutamine, 100µM non-essential amino acids (Gibco, #11140-050), 1000 units/ml Leukemia Inhibitory Factor (LIF, Millipore #ESG1107)). After 6-8 days of growth at 37˚C with 5% CO_2, blastocyst outgrowths were dissociated using 0.05% trypsin. Cells were then plated on MEFs into individual wells of a 96-well dish containing XEN derivation medium and cultured at 37˚C with 5% CO_2.Cells were screened by morphology and then passaged into 4-well wells following confluency, and then finally into 6-well wells without MEFs. For maintenance of derived cell lines, XEN cells were grown in XEN medium (MEMα, 20% fetal bovine serum, 1 mM sodium pyruvate, 100 µM β-mercaptoethanol, 2 mM L-glutamine, 100 µM non-essential amino acids) on gelatinized wells without feeders. XEN cell lines were characterized both by morphology and by expression of XEN-specific factors, assessed by RT-PCR (data not shown).

TS cells derivation, culture, and characterization was carried out as described previously (Kalantry et al., 2006).

RNA Fluorescence *in situ* Hybridization (RNA FISH) probe

Double stranded Xist probes were generated using random priming of the *Xist* gene using BioPrime DNA Labeling System (Invitrogen, #18094011). Labeling was performed at 37˚C overnight using Fluorescein-12-dUTP (Invitrogen), Cy3-dCTP (GE Healthcare, #PA53021), or Cy5-dCTP (GE Healthcare, #PA55031). Following labeling, probes were purified using a G50 Sephadex column, precipitated in a 0.3M sodium acetate solution with 200 µg yeast tRNA and 100% ethanol. Probes were spun down at 16,000x g for 20 minutes at 4˚C, then re-dissolved in 100% ethanol, with 0.01M sodium acetate. One tenth of this labeled probe stock solution was then precipitated in a 3M sodium acetate solution with 300 µg yeast tRNA (Invitrogen, #15401-029), 15 µg of mouse COT-1 DNA (Invitrogen, #18440-016), and 150 µg of sheared, boiled salmon sperm DNA (Invitrogen, #15632-011), then spun at 16,000 x g at 4˚C for 20 minutes. The pelleted probe was then washed with 70% ethanol, spun down, washed with 100% ethanol, and dried. The washed probe was then re-suspended in deionized formamide and denatured for 10 minutes at 90˚C, followed by an immediate incubation on ice for 5 minutes. A 2X hybridization solution (4X SSC, 20% dextran sulfate (Millipore, #S5030), 2.5 mg/ml purified BSA (New England BioLabs, #B90018)) was added to the denatured probe, resulting in a 1X hybridization /50% formamide solution. Probes were stored at -20˚C prior to use in IF/FISH experiments.

Immunofluorescence (IF) and IF/FISH

Cells were split onto gelatinized glass coverslips and grown to confluency (2-3 days). To permeablize, cells were incubated for 20-30 seconds in cytoskeletal buffer

(CSK: 100 mM NaCl, 300 mM sucrose, 3 mM $MgCl_2$, 10 mM PIPES pH 6.8), then for 20-30 seconds in CSK containing 0.4% Triton X-100, then again for 20-30 seconds in CSK. (*Eed*$^{-/-}$ XEN cells were treated for twice as long in the aforementioned conditions). Cells were fixed for 10 minutes in 4% paraformaldehyde, washed twice with 70% ethanol, and then stored at -20˚C in 70% ethanol.

Processed cells were rinsed three times in 1X PBS, then washed three times for 3 min each while shaking. The samples were then incubated in blocking buffer (0.5 mg/ml BSA (New England BioLabs, #B9001S), 50 µg/ml yeast tRNA (Invitrogen, #15401-029), 80 units/ml RNAseOUT (Invitrogen, #10777-019), and 0.2% Tween-20, in 1X PBS) in a humid chamber at 37˚C for 30 minutes. Following the blocking step, cells were incubated with primary antibody, diluted in blocking buffer, in a humid chamber at 37˚C for 1 hour. Next, cells were washed three times for 3 minutes each in 1X PBS, 0.2% Tween-20 while shaking. The samples were incubated again in blocking buffer for 5 minutes in the humid chamber at 37˚C, then incubated in a 1:300 dilution of fluorescently-conjugated secondary antibody (Alexa Fluor, Invitrogen), diluted in blocking buffer, for 30 minutes in the humid chamber at 37˚C. Samples were washed three times in PBS/0.2% Tween-20 as above, and then either processed for RNA FISH or mounted on microscope slides using Vectashield with DAPI (Vector Labs,#H-1200) and sealed with clear nail polish.

For IF/FISH, cells were washed for 5 minutes in 70% ethanol at room temperature, dehydrated through a series of 5 minute incubations in 85%, 95%, and 100% ethanol solutions, and then air-dried. Coverslips were then incubated with a double-stranded Xist probe and hybridized overnight at 37˚C in a humid chamber.

Following hybridization, samples were washed for 7 minutes each in a humid chamber at 39˚C 3 times with 2X SSC/50% formamide, 3 times with 2X SSC, and twice with 1X SSC, with a 1:200,000 dilution of DAPI (Invitrogen, #D21490) added to the third 2X SSC wash. Coverslips were mounted on glass slides with Vectashield (Vector Labs, #H-1000) and sealed with clear nail polish.

Microscopy

Stained cells were visualized and imaged using a Nikon Eclipse TiE inverted microscope with a Photometrics CCD camera. Images were deconvolved and uniformly processed using NIS-Elements software. Published images are maximum intensity projections of Z-stacks spanning multiple planes of focus.

Protein Lysate Collection

For whole cell extracts, cells (grown for a few days in gelatinized tissue culture plates without feeders for ES and TS cells) were washed in cold 1X PBS, then incubated in modified RIPA buffer (50 mM Tris-HCl pH 7.4, 1% NP-40, 0.25% sodium deoxycholate, 150 mM NaCl) with protease inhibitors (Complete Protease Inhibitor tablet (catalog number), 1 mM PMSF, and a 1:100 dilution of Aprotinin (EMD Millipore/Calbiochem, #616399-100KU)) for 10 minutes on ice with mild agitation. Lysates were then collected using a cell scraper and sonicated three times for 30 seconds each, with 1 minute rest periods in between. Lysates were then spun for 15 minutes at 16,000 x g at 4˚C to remove insoluble components.

Acid Extraction of Histones.

Isolation of histones was performed essentially as described in Shechter et al., 2007. Briefly, cells were pelleted, washed with 1X PBS, resuspended in hypotonic lysis buffer (10 mM Tris pH 8.0, 1 mM KCl, 1.5 mM MgCl2) with protease inhibitors (1 mM DTT, 1 mM PMSF, Complete Mini EDTA Protease Inhibitor Tablets, catalog number), rocked at 4˚C for 30 minutes, and then spun down at 10,000g for 10 min at 4˚C to pellet nuclei. Nuclei were then resuspended in 0.2M H_2SO_4 and incubated overnight at 4˚C. Histones, which were present in the supernatant, were precipitated by adding trichloroacetic acid and incubating for 30 minutes on ice. Histones were pelleted at 16,000g for 10 min at 4˚C, subjected to a series of acetone washes, and then dissolved in ddH_2O. To assess purity, 5 µg of histone samples were run on 15% polyacrylamide gels, then stained with Denville Blue Protein Stain (Denville Scientific, #E2700-SA).

Western Blotting and Quantification

For EZH2 Western blots, 30 µg of whole cell extracts were loaded in gels. For H3K27me3 Western blots, 15 µg of acid extracted histones were loaded in gels. Western blotting was performed using the antibodies listed below with the dilutions in Table 1. EZH2 Western blots were performed using HRP-labeled secondary antibodies at a dilution of 1:5000 and detected using SuperSignal West Pico Chemiluminescent Substrate (Thermo Scientific, #34079) in a G:Box iChemiXR (Syngene) with GeneSys software (v.1.2.5.0) using no light and no filter H3K27me3 and H4 Western blots were performed using fluorescently-conjugated secondary antibodies (Alexa Fluor, Invitrogen) at a dilution of 1:300 and detected/imaged using G:Box iChemiXR with the

FRLP filter and Lights Red LED (RGB) for the 647 wavelength and the SGNB filter and Lights Green LED (RGB) for the 555 wavelength. Quantification of band intensity was performed on unsaturated fluorescent images using Syngene Genetools software, and values were normalized to the intensity of the H4 loading control for each lane.

Antibodies

Table 1: The antibodies used in Western blotting and IF experiments (with dilutions)

Antibody	**Supplier**	**Raised in**	**Western Blot**	**IF**
EZH2	Cell Signaling (DC29)	Rabbit (mAb)	1:1000	1:200
H3K27me3	Millipore (ABE44)	Rabbit (pAb)	1:5000	1:5000
H3K27me3	Active Motif (39155)	Rabbit (pAb)	1:5000	1:1000
H3K27me3	Abcam (ab6002)	Mouse (mAb)	1:500	1:200
H3K27me3*	Millipore (07-449)	Rabbit (pAb)	1:2500	Still determining
EZH1	Millipore (ABE281)	Rabbit (pAb)	1:2500	N/A
EZH1	Abcam (ab137693)	Rabbit (pAb)	1:500	N/A
EZH1	Abcam (ab64850)	Rabbit (pAb)	1:250	N/A
EZH1	LS Bio (LS-C676)	Rabbit (pAb)	1:250	N/A
EZH1	LS Bio (LS-C176828)	Rabbit (pAb)	1:750	N/A
EZH1	Company (LS-C144356)	Rabbit (pAb)	1:500	N/A
EED	Millipore (09-774)	Rabbit (pAb)	1:1000	N/A
β-actin	Sigma Aldrich (A5060)	Rabbit (pAb)	1:5000	N/A
Histone H4	Cell Signaling (L64C1)	Mouse (mAb)	1:500	N/A

*Note: All experiments are in the process of being repeated with this antibody (Millipore, 07-449). So far, by Western blotting, the antibody shows the same results as the antibody described in this study (Millipore, ABE44) for all XEN cell genotypes described in the study, including *Ezh2*$^{-/-}$, *Ezh2*$^{-/-}$*;Ezh1*$^{-/-}$ and *Eed*$^{-/-}$. IF experiments with this antibody are still undergoing optimization.

RT-PCR and PCR Primers

For RT-PCR experiments, total RNA was isolated from cells using Trizol reagent (Life Technologies, #15596018) in order to do a phenol-chloroform extraction. mRNA was purified from total RNA using the Dynabeads mRNA DIRECT Micro Kit (Life

Technologies, #61012). RT-PCR was performed using Superscript III One-Step RT-PCR System with Platinum *Taq* DNA Polymerase (Life Technologies, #12574-026).

Table 2: List of Primers, sequences, and their uses.

Primer (F/R)	Sequence	Use	Figure
Ezh2-5-loxP-3 (F)	CTGGCTCTGTGGAACCAAAC	*Ezh2* PCR	5A, 8A
Ezh2-L5-loxP-1 (F)	ATGGGCCTCATAGTGACAGG	*Ezh2* PCR	5A, 8A
Enx1-3-loxP (R)	GGAGTTGCCATTCAGAGCAG	*Ezh2* PCR	5A, 8A
Ezh2delete 5-2 (F)	AACACCAAACAGTGTCCATGCTAC	Ezh2 RT-PCR	5B, 9A
Ezh2delete 3-2(R)	CTAAGGCAGCTGTTTCAGAGAGAA	Ezh2 RT-PCR	5B, 9A
Ezh1SA-1 (F)	GTACTCTTAACCACTGGACTG	*Ezh1* PCR	8B
Ezh1WT-3 (R)	GTCTTGCTATGAGGACAGGAG	*Ezh1* PCR	8B
Ezh1LACZ-2(R)	CCTGAATGGCGAATGGCGCTT	*Ezh1* PCR	8B
Ezh1ex2F (F)	CGTCTGCAGAACAGAGGTA	Ezh1 RT-PCR	9C
Ezh1ex3F (F)	GAGTATATGCGGCTTCGACA	Ezh1 RT-PCR	9C
Ezh1ex4F (F)	AAATTTTGCAAAGGTTCAAG	Ezh1 RT-PCR	9C
Ezh1ex5F (F)	TTGATGCGGTCTCTGAACAC	Ezh1 RT-PCR	9C
Ezh1ex6F (F)	TACATGGGTGACGAGGTGAA	Ezh1 RT-PCR	9A
Ezh1WalkEx8F (F)	GCAACAAAAAGAGTTCCAAG	Ezh1 RT-PCR	9C
Ezh1Setex19R (R)	CATAACAGTTGGGGTTCACT	Ezh1 RT-PCR	9A & C
Ezh1ex5R1 (R)	ATCAACATATCCTGGCTGTC	Ezh1 RT-PCR	9B
EED 5’ (F)	GGACTCATCCTCTGGTAGAGCAGC	*Eed* PCR	14A
EED 3’a (R)	TCAGCCTCAAGGGACTATCG	*Eed* PCR	14A
EED R1 (R)	TCAATTGGTGGGTTTTGGAT	*Eed* PCR	14A
EEDexon5F (F)	AACACCAGCCACCCTCTATT	Eed RT-PCR	14B
EEDexon12R (R)	ATGATGGGTCAGTGTTGTGC	Eed RT-PCR	14B

ACKNOWLDGEMENTS

I would like to thank my mentor, Sundeep Kalantry, for giving me the opportunity to work on this project and experience scientific research firsthand, as well as for the mentoring and discussions necessary for me to be able to write this thesis, and more importantly, develop as a scientist. I would like to thank Clair Harris for deriving and maintaining the cell lines used in this study, teaching me many of the skills I needed to perform the experiments, providing moral support, and for otherwise helping me out, especially when I was pressed for time while performing experiments that could not fully be completed on an undergraduate schedule. I would also like to thank the other members of the Kalantry lab for providing a fun and supportive environment in which to do this research.

I would like to thank my co-sponsor, Gyorgyi Csankovski, for guidance in the thesis process and for helpful classroom instruction. I would also like to thank Andrzej Wierzbicki for helpful classroom instruction in the field of epigenetics and for agreeing to be a reader for this thesis.

The Ezh1 mutant mice were generated at the Research Institute of Molecular Pathology (IMP, Vienna) in 2000 by Dønal O'Carroll (laboratory of Thomas Jenuwein) with the help of Maria Sibilia (laboratory of Erwin Wagner).

REFERENCES

Brown, C.J., Ballabio, A., Rupert, J.L., Lafreniere, R.G., Grompe, M., Tonlorenzi, R., and Willard, H.F. (1991). A gene from the region of the human X inactivation centre is expressed exclusively from the inactive X chromosome. *Nature* 349: 38-44.

Cao, R., Wang, L., Wang, H., Xia, L., Erdjument-Bromage, H., Tempst, P., Jones, R.S., and Zhang, Y. (2002). Role of histone H3 lysine 27 methylation in Polycomb-group silencing. *Science* 298: 1039-1043

Cao, R. and Zhang, Y. (2004). SUZ12 is required for both the histone methyltransferase activity and the silencing function of the EED-EZH2 complex. *Molecular Cell* 15: 57-67.

Cao, Q., Wang, X., Zhao, M., Yang, R., Malik, R., Qiao, Y., Poliakov, A., Yocum, A.K., Li, Y., Chen, W., Cao, X., Jiang, X., Dahiya, A., Harris, C., Feng, F.Y., Kalantry, S., Qin, Z.S., Dhanasekaran, S.M., and Chinnaiyan, A.M. (2014). The central role of EED in the orchestration of Polycomb group complexes. *Nature Communications* 5.

Da Rocha, S.T et al. (2014). Jarid2 is implicated in the initial Xist-induced targeting of PRC2 to the inactive X chromosome. *Molecular Cell* 53: 301-316.

Dillon, S.C., Zhang, X., Trievel, R.C., and Cheng, X. (2005). The SET-domain protein superfamily: protein lysine methyltransferases. *Genome Biology* 6: 227.

Egelhofer, T.A. et al. (2011). An assessment of histone-modification antibody quality. *Nature Structural and Molecular Biology* 18: 91-93.

Han, Z., Xing, X., Hu, M., Zhang, Y., Liu, P., and Chai, J. (2007). Structural basis of EZH2 recognition by EED. *Structure* 15 (10): 1306-1315.

Kalantry, S. and Magnuson, T. (2006). The Polycomb group protein EED is dispensable for the initiation of random X-chromosome inactivation. *PLoS Genetics* 2(5): e66.

Kalantry, S., Mills, K.C., Yee, D., Otte, A.P., Panning, B., and Magnuson, T. (2006). The Polycomb group protein Eed protects the inactive X-chromosome from differentiation-induced reactivation. *Nature Cell Biology* 8, 195-202.

Kleer, C.G., Cao, Q., Varambally, S., Shen, R., Ota, I., Tomlins, S.A., Ghosh, D., Sewalt, R.G.A.B., Otte, A.P., Hayes, D.F, Sabel, M.S., Livant, D., Weiss, S.J., Rubin, M.A., and Chinnaiyan, A.M. (2003). EZH2 is a marker of aggressive breast cancer and promotes neoplastic transformation of breast epithelial cells. *PNAS* 100 (20): 11606-11611.

Kouzarides, T. (2007). Chromatin modifications and their function. *Cell* 128(4): 693-705.

Kuzmichev, A., Nishioka, K., Erdjument-Bromage, H., Tempst, P., and Reinberg, D. (2002). Histone methyltransferase activity associated with a human multiprotein complex containing the Enhancer of Zeste protein. *Genes and Development* 16: 2893-2905.

Laible, G., Wolf, A., Dorn, R., Reuter, G., Nislow, C., Lebersorger, A., Popkin, D., Pillus, L., and Jenuwein, T. (1997). Mammalian homologues of the *Polycomb*-group gene *Enhancer of Zeste* mediate gene silencing in *Drosophila* heterochromatin and at *S. cerevisiae* telomeres.*The EMBO Journal* 16: 3219-3232.

Lyon, M.F. (1961). Gene action in the X-chromosome of the Mouse (*Mus musculus* L.) *Nature* 190: 372-373.

Margueron, R., Li, G., Sarma, K., Blais, A., Zavadil, J., Woodcock, C.L., Dynlacht, B.D., and Reinberg, D. (2008). Ezh1 and Ezh2 maintain repressive chromatin through different mechanisms. *Molecular Cell* 32: 503-518.

Margueron, R., Justin, N., Ohno, K., Sharpe, M.L., Son, J., Drury, W.J., Voigt, P., Martin, S.R., Taylor, W.R., De Marco, V., Pirrotta, V., Reinberg, D., and Gamblin, S.J. (2009). Role of the Polycomb protein EED in the propagation of repressive histone marks. *Nature* 461: 762-767.

Margueron, R. and Reinberg, D. (2011). The Polycomb complex PRC2 and its mark in life. *Nature* 469 (7330): 343-349.

McCabe, M.T. et al. (2012). EZH2 inhibition as a therapeutic strategy for lymphoma with EZH2-activating mutations. *Nature* 492: 108-112.

Montgomery, N.D., Yee, D., Chen, A., Kalantry, S., Chamberlain, S.J., Otte, A.P., and Magnuson, T., (2005). The murine Polycomb group protein Eed is required for histone H3 lysine-27 methylation. *Current Biology* 15 (10): 942-947.

Muller, J., Hart, C.M., Francis, N.J., Vargas, M.L., Sengupta, A., Wild, B., Miller, E.L., O'Connor, M.B., Kingston, R.E., and Simon, J.A. (2002). Histone methyltransferase activity of a *Drosophila* Polycomb group repressor complex. *Cell* 111 (2): 197-208.

Payer, B., and Lee, J.T. (2008). X chromosome dosage compensation: how mammals keep the balance. *Annual Review of Genetics* 42: 733-772.

Plath, K., Fang, J., Mlynarczyk-Evans, S.K., Cao, R., Worringer, K.A., Wang, H., de la Cruz, C.C., Otte, A.P., Panning, B., and Zhang, Y. (2003). Role of histone H3 lysine 27 methylation in X inactivation. *Science* 300:131-135.

Sewalt, R.G.A.B., van der Vlag, J., Gunster, M.J., Hamer, K.M., den Blaauwen, J.L., Satijn, D.P.E., Hendrix, T., van Driel, R., and Otte, A.P. (1998). Characterization of interactions between the mammalian Polycomb-group proteins Enx1/EZH2 and EED suggests the existence of different mammalian Polycomb-group complexes. *Molecular and Cellular Biology* 18(6): 3586-3595.

Shechter, D., Dormann, H.L., Allis, C.D., and Hake. S.B. (2007). Extraction, purification, and analysis of histones. *Nature Protocols* 2: 1445-1457.

Shen, X., Liu, Y., Hsu, Y.J., Fujiwara, Y., Kim, J., Mao, X., Yuan, G.C., and Orkin, S.H. (2008). EZH1 mediates methylation on histone H3 lysine 27 and complements EZH2 in maintaining stem cell identity and executing pluripotency. *Molecular Cell* 32: 491-502.

Shogren-Knaak, M., Ishii, H., Sun, J., Pazin, M.J., Davie, J.R., and Peterson, C.L. (2006). Histone H4-K16 acetylation controls chromatin structure and protein interactions. *Science* 311: 844-847.

Silva, J., Mak, W., Zvetkova, I., Appanah, R., Nesterova, T.B., Webster, Z., Peters, A.H.F.M., Jenuwein, T., Otte, A.P., and Brockdorff, N. (2003). Establishment of histone H3 methylation on the inactive X chromosome requires transient recruitment of Eed-Enx1 Polycomb group complexes. *Developmental Cell* 4: 481-495.

Simon, J.A. and Kingston, R.E. (2009). Mechanisms of Polycomb gene silencing: knowns and unknowns. *Nature Reviews Molecular Cell Biology* 10 (10):697-708.

Struhl, G. and Brower, D. (1982). Early role of the *esc*+ gene product in the determination of segments in Drosophila. Cell 31: 285-292.

Su, I., Basavaraj, A., Krutchinsky, A.N., Hobert, O., Ullrich, A., Chait, B.T., and Tarakhovsky, A. (2002). Ezh2 controls B cell development through histone H3 methylation and *Igh* rearrangement. *Nature Immunology* 4(2): 124-131.

Tie, F., Startton, C.A., Kurzhals, R.L., and Harte, P.J. (2007) The N terminus of *Drosophila* ESC binds directly to histone H3 and is required for E(z)-dependent trimethylation of H3 lysine 27. *Molecular and Cellular Biology* 27: 2014-2026.

Varembally, S., Dhanasekaran, S.M., Zhou, M., Barrette, T.R., Kumar-Sinha, C., Sanda, M.G., Ghosh, D., Pienta, K.J., Sewalt, R.G.A.B., Otte, A.P., Rubin, M.A., and Chinnaiyan, A.M. (2002). The Polycomb group protein EZH2 is involved in progression of prostate cancer. *Nature* 419: 624-629

Wang, J., Mager, J., Chen, Y., Schneider, E., Cross, J.C., Nagy, A., and Magnuson, T. (2001). Imprinted X inactivation maintained by a mouse *Polycomb* group gene. *Nature Genetics* 28: 371-375.

Zhao J., Sun B.K., Erwin J.A., Song J., and Lee J.T. (2008). Polycomb proteins targeted by a short repeat RNA to the mouse X chromosome. *Science* 322: 750-755.